# An Online Efficiency Optimization Strategy Based on Variable-Frequency Phase-Shift Modulation for Dual-Active-Bridge Converters

Yanxiang Yin, Wei Wang, Nan Wang, Alian Chen*
School of Control Science and Engineering, Shandong University, Jinan, China

***Abstract*-- The DC transformer (DCT) is a key equipment of the power router. To improve the DCT efficiency, this paper proposes a variable-frequency phase-shift modulation (VFPSM) strategy for the dual-active-bridge (DAB) converter which operates at the fixed voltage-transfer-ratio. The optimal switching frequency can be calculated by the VFPSM strategy online through the proposed loss model to ensure that the total of switching loss, conduction loss, and core loss is the minimum under different output powers. Besides, the frequency control and phase-shift control are decoupled by using the proposed frequency compensation factor, which would not affect the characteristics of the original DAB control method. Experimental results show that compared with conventional fix switching frequency control, the proposed VFSPM strategy can improve efficiency over a wide power range, and efficiency can be improved by up to 7.4%.**

***Index Terms*—Dual-active-bridge converter, online efficiency optimization, power router, variable-frequency phase-shift modulation.**

## I. INTRODUCTION

In recent years, the energy problem has been getting more attention. The power router is a critical equipment for efficiently using renewable energy [1]. The DC transformer is the core equipment to connect different voltage level DC buses in the power router, and its efficient operation is essential. Dual active bridge (DAB) converters are widely used in the power router due to the advantages of high efficiency, bidirectional power transmission, and high power density [2]. When the DC bus voltage is regulated by other sources, loads, or energy storage devices, the DAB only needs to adjust the transmission power, which operates at the fixed voltage-transfer-ratio, so it is imperative to optimize the efficiency of this operating condition.

Over the recent years, many papers have studied how to optimize the efficiency of DAB by expanding its soft switching range when it is running outside the fixed voltage-transfer-ratio. In [3], a proper design method of the magnetizing current in the transformer and the nonunity voltage gain conditions is proposed, which can achieve full load range ZVS for all switches in a certain voltage variation range with the single phase-shift (SPS) control to improve efficiency at light load. In [4], a double phase-shift control method using magnetizing current optimization is proposed, which significantly enlarges the soft switching range compared with SPS control, thus improving efficiency. In [5], based on the triple-phase-shift modulation, a quasi-optimal current root-mean-square (RMS) control strategy with combining the global optimal control strategy and the ZVS condition is proposed, which not only achieves All-ZVS control but also optimizes the RMS value of the inductor current, and thus the efficiency of the DAB converter is optimized. However, it does not consider the transformer core loss, and the modulation strategy is complex. In [6], a switching sequence and burst-mode strategy based on trajectory analysis is proposed, which can balance conduction loss, switching loss, and magnetic loss under light, medium, and heavy loading conditions leading to higher efficiency from light to full loading conditions. However, this variable frequency method presets different working frequencies in advance according to light, medium, and heavy loading conditions, thus it cannot achieve seamless frequency conversion and online optimization. In [7], the SPS and frequency modulation are combined to expand the range of soft switching by minimizing the circulating current, and then the efficiency is improved. However, its frequency and phase are coupled, and voltage is controlled by the feedforward method, and it needs extra compensation control. All of the above studies focus on DAB converters with wide voltage input and output. Optimization aims at achieving a wider range of soft switching to improve efficiency, and the loss of the transformer core is rarely considered. However, when operating at the fixed voltage-transfer-ratio, the DAB converters can achieve zero voltage switching (ZVS) in the almost whole load range, and these methods, which only consider ZVS and circulating current, are hard to improve the efficiency further. Overall, few articles focus on the efficiency optimization of fixed-ratio DAB converters.

At the fixed voltage-transfer-ratio, because ZVS is realized, the proportion of switching loss and core loss will decrease and increase, respectively. Hence, apart from the conduction loss and switching loss, core loss should be taken into consideration. Besides, the total loss is no longer a monotonic function of frequency, and dynamically selecting the optimal switching frequency under different powers is indispensable to further reduce the total loss and

This work was supported in part by the National Natural Science Foundation of China under Grant U2006222 and 51877128, in part by the Foundation for Innovative Research Groups of National Natural Science Foundation of China under Grant 61821004, in part by the Major Scientific and Technological Innovation Projects of Shandong Province 2019JZZY010904.

improve the efficiency of the DAB converter.

In this paper, a variable-frequency phase-shift modulation (VFPSM) is presented for the DAB operating at the fixed voltage-transfer-ratio, which can online optimize the switching frequency based on the loss model. This method comprehensively considers the switching loss, core loss, and conduction loss and can calculate the optimal frequency corresponding to different output power in real time, thus improving the efficiency of the converter in the whole load range. In addition, in the proposed strategy, frequency control and phase-shift control are decoupled, so the PI controller can maximize its performance and improve the dynamic response of the DAB converter.

## II. Topology and Power Transfer Characteristics of the DAB Converter

The topology of the DAB converter is shown in Fig. 1. The primary side H-bridge consists of four MOSFETs $S_1$-$S_4$. The secondary side H-bridge consists of four MOSFETs $S_5$-$S_8$. $V_{AB}$ and $V_{CD}$ are the voltage between the midpoint of each H bridge. The value of $L_s$ is the sum of transformer leakage inductance and extern inductance. The transformer magnetizing inductance is $L_m$, the turn ratio is n, the equivalent resistance normalized to the primary side is $R$, and the current flowing through the inductance is $I_L$. The DAB converter power is controlled by the phase-shift angle $D$ between the primary and secondary bridges.

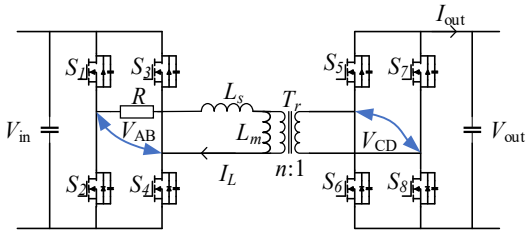


Fig. 1. The circuit topology of DAB.

When the DAB converter losses are ignored and the transformer magnetizing inductance is large enough, the key DAB converter phase-shift modulation (PSM) waveforms are shown in Fig. 2. The simplified transfer power equation of the DAB converter can be obtained:

$$P = \frac{nV_{in}V_{out}}{2f_sL_s}D\left(1-|D|\right),\quad D\in[-0.5,0.5]. \tag{1}$$

where $V_{in}$ and $V_{out}$ are input voltage and output voltage, respectively. $f_s = 1/2T_s$ is the switching frequency.

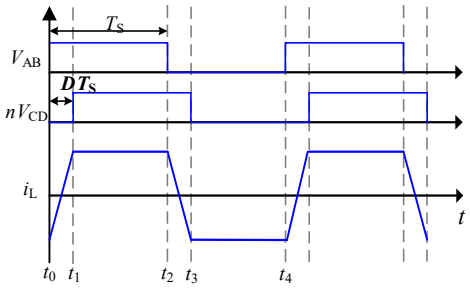


Fig. 2. Idealized operating waveforms of the DAB converter when $V_{in}=nV_{out}$. The power flow is from $V_{in}$ to $V_{out}$.

## III. The DAB Converter Losses Model and VFPSM Strategy

The DAB converter loss is optimized using the general power flow equation (1). The loss model considers the switching loss of semiconductor devices, core loss of transformers, and conduction loss of the current path.

### A. Converter Loss Model

For the switching devices in the DAB, when the switching frequency is high, hard switching will lead to high losses, while soft switching technology can effectively reduce the switching loss. Therefore, the SPS controlled DAB should ensure soft switching is achieved. At the fixed voltage-transfer-ratio, the ZVS turn-on is naturally achieved in the whole load range, and in this paper, the proposed DAB loss model is based on this operating condition.

In the proposed loss model, the turn-on loss is small and ignored. The turn-off loss can be calculated by the measured waveform and equation (2) or estimated by the datasheet and equation (3) provided by the manufacturer [8]. In order to realize the online calculation of turn-off loss, the latter method is adopted in this paper, and the accuracy of this method is verified by experiments.

$$E_{off\_measure} = \int_0^{t_{off}} i_D(\tau)v_{DS}(\tau)d\tau \tag{2}$$

$$E_{off\_estimate} = E_{off,datasheet}(400\text{ V}, I_D)\cdot\frac{V_{DS}}{400\text{ V}} \tag{3}$$

The transformer core loss is also a significant component of the DAB converter losses. Generally, the Steinmetz equation is used to estimate the core loss of the transformer, but it only shows good accuracy under sinusoidal excitation. For DAB converters, it is usually triangular wave excitation. Therefore, the improved general Steinmetz equation (iGES) [9] is used to estimate the core loss in this paper. The core loss of the transformer can be fitted according to the datasheet and equations (4) and (5). When the stray inductance of the transformer is ignored, the peak magnetic flux density $B_{Tr}$ can be estimated by equation (6) [10].

$$P_{core} = V_{Tr}\cdot\frac{1}{T_s}\int_0^{T_s} k_i\left|\frac{dB_{Tr}}{dT_s}\right|^{\alpha}\left|\Delta B_{Tr}\right|^{\beta-\alpha}dt \tag{4}$$

$$k_i = \frac{C_m}{(2\pi)^{\alpha-1}\int_0^{2\pi}\left|\cos\theta\right|^{\alpha}2^{\beta-\alpha}d\theta} \tag{5}$$

$$B_{Tr} \approx V_{out}/(4f_sN_2A_{Tr}) \tag{6}$$

where $V_{Tr}$ is the transformer effective volume, $A_{Tr}$ is the transformer effective area, $C_m$, $\alpha$, $\beta$ are the fitting coefficients, and $N_2$ is the number of secondary side turns.

In addition, the conduction loss of the converter is also a vital part. The conduction loss usually acts on the resistance in the form of heat loss, which can be estimated from $I_{RMS}^2R$, where $R$ is the lumped equivalent resistance of the converter, mainly including the on-resistance of the

primary and secondary switches and the equivalent resistance of the inductance winding, transformer winding and other lines. $I_{RMS}$ is the RMS value of primary inductance current, which can be deduced according to the working principle of DAB, as shown in Fig. 2. Since DAB works at the fixed voltage-transfer-ratio, to achieve ZVS in the entire load range, the transformer ratio can be designed as the voltage-transfer-ratio of the primary and secondary sides, i.e., $V_{in}/V_{out}$=n. According to Fig. 2, the current flowing through the inductance $L_s$ can be calculated (only the first half cycle is given due to symmetry):

$$i_L(t) = i_L(t_0) + \frac{V_{in} + nV_{out}}{L_s}(t - t_0), t_0 \le t < t_1 \quad (7)$$

$$i_L(t) = i_L(t_1) + \frac{V_{in} - nV_{out}}{L_s}(t - t_1), t_1 \le t < t_2 \quad (8)$$

$$i_L(t_2) = -i_L(t_0). \quad (9)$$

Then the RMS value of the current $I_{RMS}$ and the conduction loss $P_{cond}$ can be obtained from the above equation.

$$I_{RMS} = \sqrt{\frac{1}{t_2}\int_{t_0}^{t_2} i_L(t)^2 dt} = \frac{V_{in}D}{2f_sL_s}\sqrt{\frac{3-2D}{3}} \quad (10)$$

$$P_{cond} = I_{RMS}^2 \cdot R = \frac{3V_{in}^2D^2 - 2V_{in}^2D^3}{12f_s^2L_s^2} \cdot R \quad (11)$$

According to the above equation, the expression of total loss $P_{total}$ can be derived:

$$P_{total} = P_{cond} + P_{core} + P_{off} = \frac{3V_{in}^2D^2 - 2V_{in}^2D^3}{12f_s^2L_s^2} \cdot R + P_{core} + f_s \cdot E_{off\_estimate} \quad (12)$$

At this time, when using the above equation for efficiency optimization, it is necessary to consider the phase shift angle $D$ and switching frequency $f_s$ simultaneously, which is a two-dimensional optimization. This not only brings difficulties to the control and optimization process but also easily leads to power transmission imbalance, thus introducing additional compensation mechanisms. Therefore, this paper uses the general power flow equation to realize the decoupling control of $D$ and $f_s$ in the efficiency optimization process. According to equation (1), when power flows forward, the relationship among phase shift angle $D$ and switching frequency $f_s$ and transmission power $P$ can be derived in equation (13).

$$D = \frac{1}{2} - \sqrt{\frac{1}{4} - \frac{2f_sL_sP}{V_{in}^2}} \quad (13)$$

According to equations (12) and (13), the expression of total loss $P_{total\_loss}$ under different output power $P$ can be derived in equation (14).

After decoupling, it can be seen that when the converter parameters and input voltage are fixed, its loss is only related to the switching frequency and transmission power. Fig. 3 shows the relationship between the different converter losses and switching frequency when the output power is 90W.

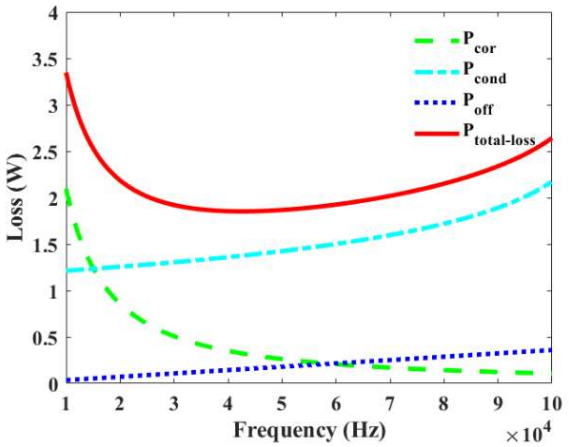


Fig. 3. The relationship between the different converter losses and switching frequency when the output power is 90W.

It can be seen from Fig. 3 that the core loss $P_{cor}$ decreases with the increase of switching frequency $f_s$. On the contrary, the conduction loss $P_{cond}$ and the turn-off loss $P_{off}$ increase with the increase of $f_s$. Therefore, there is an optimal frequency to minimize the total losses, which can also be seen in Fig. 3. In addition, the optimal frequency will also change according to the change of the output power, as shown in Fig. 4, where the black dotted line represents the relationship between the converter total loss and the switching frequency when the output power is constant, and the output power has been marked in the figure. It can be seen from Fig. 4 that with the increase in power level, the optimal switching frequency will gradually decrease. This is because the core loss is only related to the switching frequency, while the conduction loss increases with the increase of power, which leads to the dominant conduction loss in the total loss when the output power is heavy, so a lower switching frequency is required to achieve better efficiency. Based on the above analysis, there is an optimal design trade-off among switching loss, conduction loss, and core loss at different load power and switching frequencies. Therefore, searching for optimal frequency can improve the efficiency of the converter.

$$P_{total\_loss} = P_{cond} + P_{core} + P_{off} = \frac{V_{in}^2}{12f_s^2L_s^2}\left(3\left(1/2 - \sqrt{1/4 - 2f_sL_sP/V_{in}^2}\right)^2 - 2\left(1/2 - \sqrt{1/4 - 2f_sL_sP/V_{in}^2}\right)^3\right) \cdot R + P_{core} + P_{off} \quad (14)$$

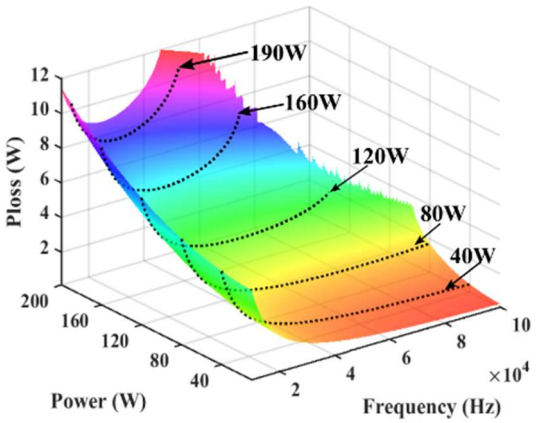


Fig. 4. The relationship among converter total loss, switching frequency, and output power.

### B. VFPSM Strategy

The control block diagram of the VFPSM algorithm is shown in Fig. 5. The decoupled switching frequency and phase-shifting angle can be controlled separately by a two-part controller. The proposed VFPSM strategy can be divided into the VFM and PSM strategies, which control the switching frequency and phase shift angle, respectively. For the DAB converter operating at the fixed voltage-transfer-ratio, the ZVS of the entire load range can be achieved by using the single-phase shift modulation strategy, and it is simple and easy to achieve compared with the multi-phase shift modulation strategy. Equation (14) shows that when the external input and topological parameters are fixed, the loss is only related to the switching frequency, while the variable frequency modulation (VFM) algorithm finds the optimal switching frequency by minimizing $P_{\text{total\_loss}}$ and uses this frequency output as the frequency reference of the PSM algorithm, as shown in Fig. 6. Due to the complexity of equation (14), it is difficult to find the analytical expressions of switching frequency and output power under the minimum total loss. Therefore, an online optimization method is needed. After the output power and output current are collected, the output power is calculated, and the switching frequency used at the next switching cycle is predicted. Since the optimization of efficiency does not require a fast speed and considers the stability of the system and the computational power of the controller used, this paper takes 100Hz as the minimum step size, namely $\Delta$= 100Hz, to predict the five discrete points of the next cycle, as shown in Fig. 7. For each cycle, fs that minimizes $P_{\text{total\_loss}}$ is selected as the switching frequency of the next cycle. After several cycles, the optimal frequency that minimizes the total loss can be found.

It is worth mentioning that after obtaining the optimal switching frequency through the proposed VFM strategy, in order not to change the control characteristics of the original controller, it is necessary to add a frequency compensation factor for the original system. After the simulation, the dynamic response characteristics of the original system can be effectively improved by introducing this factor.

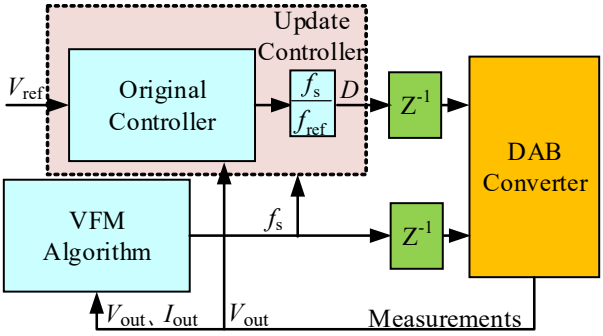


Fig. 5. The control block diagram of VFPSM.

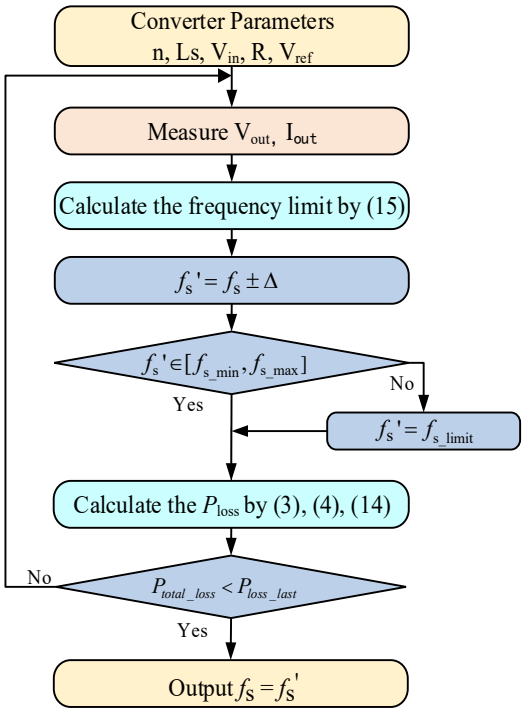


Fig. 6. VFM process flowchart.

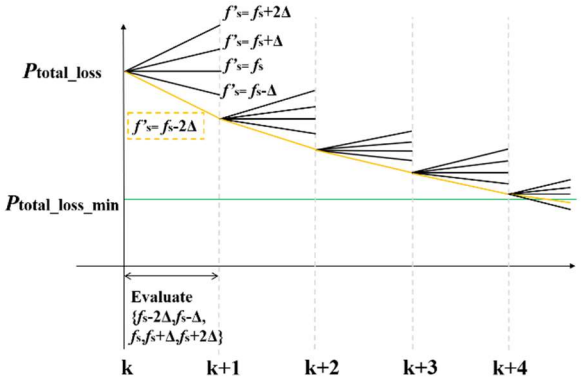


Fig. 7. Operating principle of the proposed VFM.

The switching frequency of the DAB converter needs to be limited. If the frequency is too low, it may cause the magnetic saturation of the transformer. If the switching frequency is too high, the control cycle of the actual controller may exceed one switching cycle, which will affect the original dynamic characteristics of the converter.

In addition, when the switching frequency is too high, the transmission power level of the converter will be limited, and the drive loss will increase. Therefore, considering the above factors, the switching frequency range can be obtained by (15).

$$f_{s\_max} = \min[\frac{nV_{in}V_{out}}{8L_sP}, 100\text{kHz}] \qquad (15)$$
$$f_s \in [20\text{kHz}, f_{s\_max}]$$

## IV. Experimental Results

To verify the effectiveness of the proposed VFPSM strategy, a 200W DAB prototype using TI microcontroller TMS320F28379D is built, as shown in Fig. 8. The resistance is measured by UT620C micro ohm meter. An EE50 magnetic core with the material PC40 is used to construct the transformer. For the windings, Litz wire is used to minimize the skin and proximity effect conductor losses. The component parameters are given in Table I.

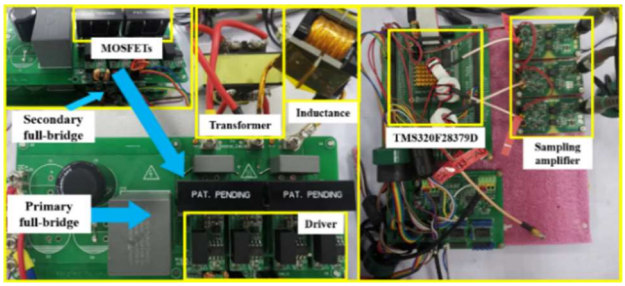

Fig. 8. DAB laboratory prototype.

TABLE I
Component Values for The DAB Prototype

| Symbol | Definition | Value |
|---|---|---|
| $V_{in}$ | Input voltage | 60V |
| $V_{out}$ | Output voltage | 40V |
| $V_{Tr}$ | Transformer effective volume | 21600mm$^3$ |
| $A_{Tr}$ | Transformer effective area | 226mm$^2$ |
| $C_m$ | Fitting coefficient | 0.027kW/m$^3$ |
| $\alpha$ | Fitting coefficient | 1.21 |
| $\beta$ | Fitting coefficient | 2.5 |
| $n$ | Turns-ratio | 15:10 |
| $f_s$ | Switching frequency | 20k~100kHz |
| $L_s$ | Leakage inductance | 46$\mu$H |
| $S_1$-$S_8$ | SiC MOSFET | C3M0060065K |
| $R$ | Equivalent resistance | 0.5225Ω |

For the turn-off loss, it is first estimated through the datasheet and equation (3). It can be seen from the data table that under the test condition of $V_{DD}$=400V and $I_{DS}$=13.2 A, when the junction temperature is 25-175 ℃, the turn-off loss changes little. Under the test condition of T=25 ℃ $V_{DD}$=400 V, when $I_{DS}$ is 5-20 A, its turn-off loss changes little. Therefore, the turn-off loss can be estimated accurately through the data table and equation (3). The estimated $E_{off\_estimate}$ is only 0.6 $\mu$J when the output power is 200W. Then, the turn-off loss is measured by Fig. 9 turn-off waveform of the MOSFET C3M0060065K used in this paper. According to the measured waveform and equation (2) the measured $E_{off\_measure}$ is 1.0 $\mu$J. However, [11] proved that this estimation method considers the energy stored in MOSFET $C_{oss}$. In the case of soft switching, this energy will not be dissipated entirely but will provide part of the energy for the next cycle of ZVS so that the resulting turn-off loss will be overestimated. Therefore, comparing the two methods, it is found that equation (3) is more accurate and easier to realize online calculation.

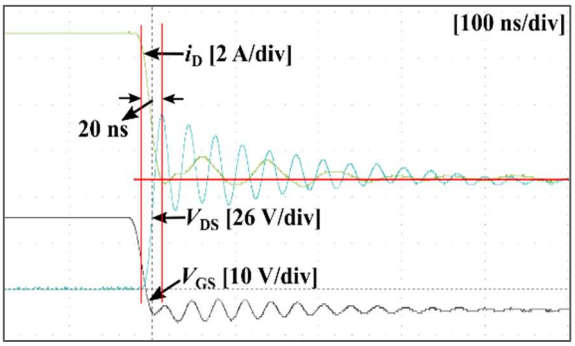

Fig. 9. Measured turn-off waveforms of the SiC MOSFET C3M0060065K.

Fig. 10 shows the transient simulation results when operating at a fixed frequency of 50kHz and VFPSM control with a frequency compensation factor. It can be seen from the figure that the proposed strategy improves the dynamic characteristics of the original system.

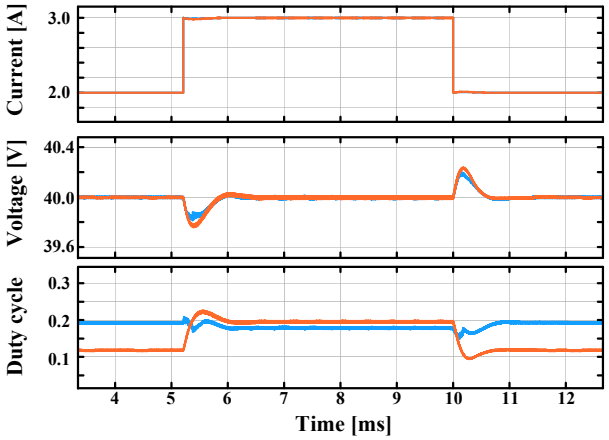

Fig. 10. The simulation waveforms of transient response.

Fig. 11 shows the optimal frequency points calculated by MATLAB corresponding to different power and the operating switching frequencies obtained by the VFPSM algorithm during the experiment. The results are almost identical, so the VFPSM algorithm can achieve an excellent online optimization function. It can be seen from the diagram that the optimal switching frequency decreases with the increase of power level, which indicates that the core loss plays a dominant role in transformer loss under light load, and conduction loss plays a dominant role under heavy load. Therefore, the converter efficiency can be effectively improved by operating at the optimal frequency, and the efficiency curve is shown in Fig. 12. This paper compares the VFPSM strategy and fixed frequency control efficiency. The fixed frequency strategy considers 20k, 50k, and 100kHz, respectively. It can be seen from the diagram that the VFPSM strategy proposed in this paper dramatically improves the power transfer level of the converter when the switching frequency is

100kHz. Compared with 50kHz, the VFPSM strategy improves the power transmission level and efficiency during heavy load, which is 2.6% higher at 180W output power. Compared with 20kHz, the VFPSM strategy can significantly improve the efficiency of its light load, which is 7.4% higher at 10W output power. The VFPSM strategy achieves the highest efficiency of 97.6% when the output power of the converter is 40W.

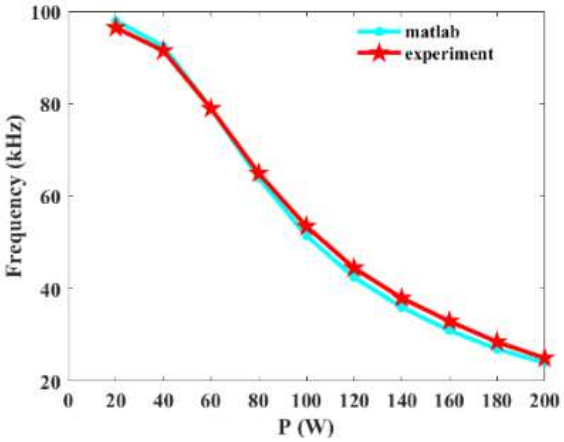


Fig. 11. Comparison between optimal frequency calculated by MATLAB and operating switching frequency in experiment with VFPSM.

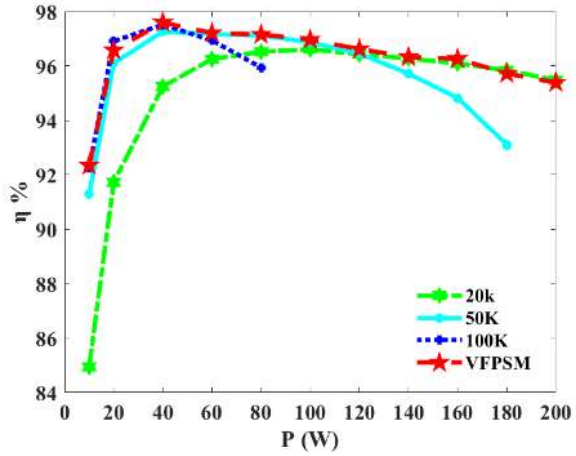


Fig. 12. Measured efficiency curves for the VFPSM and fixed frequency control at different output power.

## V. Conclusion

This paper proposed a VFPSM algorithm to improve the efficiency of a fixed-ratio DAB converter. The detailed loss model, which is only related to the switching frequency variable, is given first. Then using this model, the proposed strategy can online search for the optimal switching frequency to minimize the total loss. The switching frequency and the phase shift used in this paper are decoupled. Therefore, the PI controller can keep the original controller dynamic characteristics by adding the frequency compensation factor to its output. Experiments show that the proposed VFPSM strategy can effectively improve the efficiency and dynamic response compared with the fixed frequency strategy.

## References


[1] A. Q. Huang, M. L. Crow, G. T. Heydt, J. P. Zheng and S. J. Dale, "The Future Renewable Electric Energy Delivery and Management (FREEDM) System: The Energy Internet," *Proceedings of the IEEE*, vol. 99, no. 1, pp. 133-148, Jan. 2011.

[2] R. W. A. A. De Doncker, D. M. Divan and M. H. Kheraluwala, "A three-phase soft-switched high-power-density DC/DC converter for high-power applications," in *IEEE Transactions on Industry Applications*, vol. 27, no. 1, pp. 63-73, Jan.-Feb. 1991.

[3] X. Chen, G. Xu, H. Han, D. Liu, Y. Sun and M. Su, "Light-Load Efficiency Enhancement of High-Frequency Dual-Active-Bridge Converter Under SPS Control," in *IEEE Transactions on Industrial Electronics*, vol. 68, no. 12, pp. 12941-12946, Dec. 2021.

[4] L. Li, G. Xu, and M. Su, "An Optimized DPS Control for Dual-Active-Bridge Converters to Secure Full-Load-Range ZVS With Low Current Stress," in *IEEE Transactions on Transportation Electrification*, vol. 8, no. 1, pp. 1389-1400, Mar. 2022.

[5] H. Yu *et al.*, "Globally Unified ZVS and Quasi-Optimal Minimum Conduction Loss Modulation of DAB Converters," in *IEEE Transactions on Transportation Electrification*, vol. 8, no. 3, pp. 3989-4000, Sept. 2022, doi: 10.1109/TTE.2021.3131192.

[6] G. G. Oggier and M. Ordonez, "High-Efficiency DAB Converter Using Switching Sequences and Burst Mode," in *IEEE Transactions on Power Electronics*, vol. 31, no. 3, pp. 2069-2082, March 2016.

[7] J. Hiltunen, V. Väisänen, R. Juntunen and P. Silventoinen, "Variable-Frequency Phase Shift Modulation of a Dual Active Bridge Converter," in *IEEE Transactions on Power Electronics*, vol. 30, no. 12, pp. 7138-7148, Dec. 2015.

[8] F. Krismer, J. Biela and J. W. Kolar, "A comparative evaluation of isolated bi-directional DC/DC converters with wide input and output voltage range," *Fourtieth IAS Annual Meeting. Conference Record of the 2005 Industry Applications Conference*, 2005, pp. 599-606 vol. 1.

[9] K. Venkatachalam, C. R. Sullivan, T. Abdallah and H. Tacca, "Accurate prediction of ferrite core loss with nonsinusoidal waveforms using only Steinmetz parameters," *2002 IEEE Workshop on Computers in Power Electronics, 2002. Proceedings.*, Mayaguez, PR, USA, 2002, pp. 36-41.

[10] F. Krismer and J. W. Kolar, "Accurate Power Loss Model Derivation of a High-Current Dual Active Bridge Converter for an Automotive Application," in *IEEE Transactions on Industrial Electronics*, vol. 57, no. 3, pp. 881-891, Mar. 2010.

[11] S. K. Roy and K. Basu, "Analytical Model to Study Turn-OFF Soft Switching Dynamics of SiC MOSFET in a Half-Bridge Configuration," in *IEEE Transactions on Power Electronics*, vol. 36, no. 11, pp. 13039-13056, Nov. 2021.